

## Adjoint-enabled Uncertainty Quantification for Satellite Shield Designs

Brian M. Adams, Shawn D. Pautz, Laura P. Swiler, Brian C. Franke, and Ethan L. Blansett

Sandia National Laboratories, P.O. Box 5800, MS-1318, Albuquerque, NM, 87185, briadam@sandia.gov

**Abstract** – Radiation shields afford satellite microelectronics critical protection, but their weight can increase launch costs or limit capability. Automated transport simulation-based design optimization, particularly risk-informed design, helps designers explore virtual prototypes that meet mission requirements, including performing in the face of manufacturing and space radiation environment uncertainty. This paper focuses on adjoint-based sensitivities of transport simulation responses to design or uncertain parameters, and their role in efficient uncertainty analysis. Particular emphasis is placed on gradient-enabled reliability and polynomial chaos methods for their advantages over Monte Carlo and basic first-order uncertainty propagation. When married with optimization algorithms, these ultimately facilitate robust design accounting for uncertainty, resulting in less conservative, more cost-effective designs.

### I. INTRODUCTION

Satellites orbiting Earth are subject to harsh radiation environments primarily due to magnetically trapped electrons and protons, protons from solar flares, and cosmic rays. System designers typically use unhardened commercial off-the-shelf microelectronics due to cost, flexibility, and capability benefits. These electronics and other system components therefore require radiation shielding sufficient for the anticipated mission characteristics, such as service altitude, duration, and solar cycles and flares. To meet strict weight and space constraints, the shield mass must be minimal, while affording required electronics robustness to the intense and variable space radiation environment.

Optimal shield design can be non-intuitive as inelastic/elastic scattering and production/absorption of bremsstrahlung differentially affect electron and proton transport. For example, while a single low-Z (atomic number) shield is most effective for protons alone, graded-Z shields are considerably more effective for the combined electron/proton environment [1]. Our companion paper [2] describes an automated adjoint-enabled shield design optimization process that uses a deterministic radiation transport simulator to select optimal materials and layer thicknesses for such a graded-Z shield.

Shields must meet radiation dose limits for nominal design conditions, and also perform in an uncertain, temporally varying, radiation environment, and in the face of manufacturing variability, for example when using composites or advanced manufacturing processes. This paper focuses on applying global forward uncertainty quantification (UQ) algorithms to an adjoint-enabled radiation transport code, to predict the effect of such uncertainties on shield performance. By understanding these effects early in a risk-informed design process, or ultimately, integrating them into an automated simulation-based robust design process, designers should be able to be less conservative in meeting probabilistic requirements. To make such analyses practical, parametric design optimization and

UQ must be computationally efficient. This paper demonstrates potential efficiency gains from using adjoint-based sensitivities in combination with advanced UQ methods.

### II. DESCRIPTION OF THE ACTUAL WORK

In this work, we derive and implement adjoint-based sensitivities of radiation transport responses, such as component dose, to common shield design factors such as material composition, layer geometry, and source spectrum. Such local (at a point in parameter space) derivatives are often used for basic first-order forward uncertainty propagation, for example to transform a multivariate normal cross section covariance matrix to a corresponding response covariance matrix.

The present exposition emphasizes novel combination of these sensitivities with derivative-enhanced UQ methods including reliability and polynomial chaos expansion methods to demonstrate potential cost savings over Monte Carlo sampling, together with accuracy advantages over basic first-order UQ approaches. Their joint application is demonstrated in a representative radiation shield uncertainty quantification analysis.

#### 1. Adjoint-based Parameter Sensitivities

To model satellite electron/proton shields and expected dose to silicon components of interest, we consider the familiar Boltzmann transport equation (1a) with source term  $q$  and boundary conditions given by (1b).

$$\Omega \cdot \nabla \psi + \sigma_t(r, E)\psi = \int_{E'} dE' \int_{4\pi} d\Omega' \sigma_s(r, \Omega' \rightarrow \Omega, E' \rightarrow E)\psi(r, \Omega', E') + q \quad (1a)$$

$$\psi = \psi_b(r, \Omega, E), \{r \in \partial D | \Omega \cdot \vec{n} < 0\} \quad (1b)$$

Shield design and uncertainty quantification focus on derived quantities of interest, such as an integral response  $g$

$$g = \int_D dr \int_E dE \int_{4\pi} d\Omega \psi(r, \Omega, E) q^\dagger(r, E). \quad (2)$$

The functional  $q^\dagger$  is chosen to measure the response of interest, for example,  $q^\dagger = \sigma_d(r, E)/V$  to yield component dose.

To enable efficient design optimization and uncertainty quantification, we leverage transport community advances in adjoint formulations for sensitivities, for example as described in [3, 4]. The relevant derivations are summarized here; additional details can be found in [2] and [4].

Consider (1a) in more succinct notation using streaming ( $L$ ), collision ( $C$ ), and scattering ( $S$ ) operators

$$L\psi + C\psi = S\psi + q, \quad (3)$$

together with the inner product  $\langle \cdot, \cdot \rangle$  induced by the integrals over space  $D$ , energy  $E$ , and direction  $\Omega$  shown in (2). We form a Lagrangian

$$\mathcal{L} = \langle \psi, q^\dagger \rangle - \langle \psi^\dagger, L\psi + C\psi - S\psi - q \rangle \quad (4)$$

and note that when the forward transport equation (3) is satisfied, (4) reduces to the integral response  $g$  of interest. Differentiating the Lagrangian with respect to an arbitrary input parameter  $p$  yields

$$\frac{d\mathcal{L}}{dp} = \frac{\partial \mathcal{L}}{\partial p} + \frac{\partial \mathcal{L}}{\partial \psi} \frac{\partial \psi}{\partial p}. \quad (5)$$

By requiring that  $\psi$  satisfy the forward transport equation (3) and  $\psi^\dagger$  satisfy the corresponding adjoint transport equation

$$(L^\dagger + C^\dagger - S^\dagger)\psi^\dagger = q^\dagger, \quad (6)$$

we find (details in [2]) that

$$\frac{d\mathcal{L}}{dp} = \left[ \left\langle \psi, \frac{\partial q^\dagger}{\partial p} \right\rangle + \left\langle \psi^\dagger, \frac{\partial q}{\partial p} \right\rangle - \left\langle \psi^\dagger, \left( \frac{\partial}{\partial p} (L + C - S) \right) \psi \right\rangle \right] = \frac{dg}{dp}. \quad (7)$$

Hence, the sensitivity of the response  $g$  to any parameter  $p$  depends on the derivatives of sources and operators, but the sensitivity with respect to any parameter can be computed from inner products involving the same forward and adjoint flux solutions. So response derivatives with respect to a potentially large number of parameters only require two transport solves and the modest computational cost of the inner products in (7).

The calculation of sensitivities (7) for specific parameters of interest is detailed in [2]. For example, the

sensitivity of the response  $g$  to shield material composition requires expressing the operators  $C$  and  $S$  in terms of the multigroup approximation and differentiating them with respect to material volume fractions. Similarly,  $C$ ,  $S$ , and  $q^\dagger$  can be differentiated with respect to parameterized material interface locations, resulting in sensitivities to geometry or component location. For the computational studies shown below, forward (3) and adjoint (6) transport solves were conducted with the SCEPTRE deterministic radiation transport code [5], and adjoint-based sensitivities to design parameters (as well as to source spectra) were newly implemented in and evaluated with companion post-processing tools.

## 2. Uncertainty Quantification Methods

Parametric forward uncertainty quantification assumes distributions on the uncertain simulation input parameters  $u$ , runs one or more code calculations over the parameter space, and calculates statistics such as moments or probability/response level pairs (cumulative distribution functions) on simulation responses of interest  $g(u)$ . These statistics can then be used to understand the typical mean or median performance of the system, variability or spread in performance, or the likelihood of exceeding design requirements. We focus here on three classes of global parametric UQ methods, which attempt to assess the influence of input parameter distributions considered over their full support. Some are based on response values only, while others can take advantage of the response value and its gradient with respect to uncertain parameters  $u$  at each point evaluated in the parameter space. A more detailed summary of these methods, with references, can be found in [6].

In **Monte Carlo sampling**, including the Latin hypercube variant used here, values of the input parameters are randomly drawn from the specified input probability distributions. The  $N$  (function value-only) simulation runs at these values can then all be performed concurrently. Statistics such as sample moments and percentiles are calculated directly from the resulting ensemble, for example, mean and standard deviation:

$$\mu_g = \frac{1}{N} \sum_i g(u^i), \text{ and} \quad (8a)$$

$$\sigma_g = \sqrt{\frac{1}{N} \sum_i (g(u^i) - \mu_g)^2}. \quad (8b)$$

Latin hypercube sampling (LHS) has several advantages over pure Monte Carlo, including sampling from equiprobable one-dimensional strata commensurate with the input distributions to better spread the points, well-mixed multi-dimensional samples that respect correlations, and greater efficiency in estimating moment statistics. While robust and easy to understand, Monte Carlo methods converge statistics slowly, e.g., halving the error in a mean estimate requires quadruple the number of model evaluations,

and thousands to millions of samples may be necessary to resolve a tail probability.

**Reliability methods** are often more efficient at calculating specific probability or response levels. They address questions such as “What is the probability of the response  $g(u)$  being less than  $g_{target}$  (typically a failure threshold) or “What is the maximal response corresponding to a 0.99 probability?” Among reliability methods, mean value is the cheapest and most approximate. A single evaluation of the computational model and its derivatives at the uncertain variable means are used to estimate any moments or probability levels. For example, in first-order mean value, the response mean and standard deviation are calculated at the uncertain variable means as:

$$\mu_g = g(\mu_u) \quad (9a)$$

$$Cov(g) = \nabla_u g(\mu_u)^T Cov(u) \nabla_u g(\mu_u) \quad (9b)$$

The first-order covariance estimate in (9b) is often colloquially referred to as the “sandwich” formula or first-order propagation of variance. It is commonly used to assess the influence of variances and covariances associated with multi-group cross section data  $u$  on a transport response of interest,  $g$ .

Most probable point search methods, another class of gradient-based reliability methods, reformulate the UQ problem as an optimization problem. Given a response level of interest  $g_{target}$ , for example  $dose = 10$  krad, an optimization solver finds the most probable point (MPP) in input space  $u$  that gives rise to that target:

$$\min_u u^T u \quad (10a)$$

$$s.t. g(u) = g_{target} \quad (10b)$$

Then probabilities are calculated by (optionally forming an approximation and) integrating about the MPP. Reliability methods typically use gradient-based optimization (nonlinear programming) solvers, such as sequential quadratic programming (SQP), to solve the transport simulation-constrained optimization problem (10), and thus directly take advantage of adjoint derivatives of the response QoIs during the solution process.

**Polynomial chaos expansions** (PCE) approximate the response function  $g(u)$  with an orthogonal polynomial expansion (11a), where the polynomials  $\phi_j(u)$  are tailored to the uncertain variable distributions to accelerate convergence.

$$g(u) \approx \sum_j c_j \phi_j(u) \quad (11a)$$

$$\frac{\partial g}{\partial u}(u) \approx \sum_j c_j \frac{\partial \phi_j}{\partial u}(u) \quad (11b)$$

The coefficients of the approximation  $c_j$  may be estimated with a number of techniques. When using regression and related approaches, the approximation and its analytic derivative (11b) can be trained with both function value  $g(u^i)$  and gradient  $\frac{\partial g}{\partial u}(u^i)$  information from each simulation sample point  $i = 1, \dots, N$ .

Once the approximation is constructed, moments can be calculated explicitly from the functional form, appealing to the orthogonality of the basis. When the response  $g(u)$  is well-approximated by the PCE, highly accurate statistics of it can be obtained.

### 3. Satellite UQ Problem Description

Consider a satellite to be flown in a 3000km circular equatorial orbit, with the surrounding radiation environment defined by the Spensvis AE8 and AP8 models [7]. Assume that the design optimization process described in our companion paper [2] was used with an adjoint-enabled radiation transport code to find the best performing shield. The designer now wishes to predict the optimal shield’s performance given uncertainties in the radiation source spectra, assumed transport cross section uncertainties, material composition, and manufacturing processes.

Figure 1 shows the simplified one-dimensional slab (infinite in other directions) geometry analyzed for this scenario. The electron and proton radiation source is imposed on the left boundary, while vacuum is prescribed on the right. The shield is comprised of a 30 mil aluminum casing, followed by three 5 mm shield layers, protecting the epoxy-embedded silicon representing microelectronics.

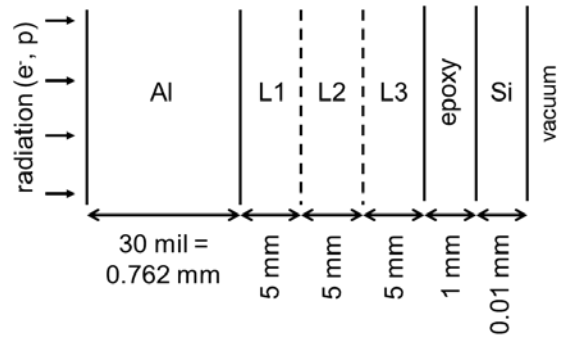


Fig. 1. Diagram of satellite shielding problem (not to scale). Compositions of layers L1, L2, and L3 are shown in Table I.

The optimal amount of uniformly mixed ultra-high molecular weight polyethylene (UHMWPE) and Ta comprising each of layers L1, L2, and L3 was automatically determined by the methods in [2]. The designed (nominal) values of these material amounts are shown in the mean column of Table I. (Note that this design exploration took advantage of the one-dimensional geometry and fixed each layer thickness at arbitrary nominal values. The densities

resulting from the optimization may therefore not be physical, but can be readily rescaled based on thickness.)

Table I. Optimal shield layer compositions, with prescribed uncertainties

Layer: Mixture	mean $\mu$ (g/cm <sup>2</sup> )	standard deviation $\sigma$ (g/cm <sup>2</sup> )
L1: UHMWPE	3.4424e+00	1.7212e-01
L1: Ta	1.3198e-02	6.5992e-04
L2: UHMWPE	3.6750e+00	1.8375e-01
L2: Ta	6.1353e-03	3.0677e-04
L3: UHMWPE	4.8077e+00	2.4039e-01
L3: Ta	9.7317e-02	4.8658e-03

The uncertainty quantification demonstration presented here addresses uncertainty in the composite material manufacturing process. The as-manufactured material densities are assumed to follow a normal distribution with means and standard deviations shown in Table I, where the standard deviations  $\sigma$  are taken to be 5% of nominal (mean  $\mu$ ). The distributions are truncated below at zero to enforce nonnegative material density.

### III. RESULTS

Dakota-based [6] forward uncertainty quantification studies using each of the methods described in Section II.2. were conducted on the satellite demonstration problem, using the SCEPTRE deterministic radiation transport code [5] and associated adjoint post-processing tools. LHS samples of sizes  $N = 5, 10, 15, 20, 25, 50, 100, 200, 400, 800, 1600,$  and 3200 were generated with both function values and adjoint-based gradients. Owing to the regression training approach used, the same datasets can be used to directly compute sample statistics and to train function value-only (PCEf) and gradient-enhanced (PCEg) PCEs. Gradient-based mean-value (MV) and most probable point (MPP) reliability studies were conducted as well.

The (relative) computational cost of the methods is summarized in Table II, where the 1.75 cost of a forward + adjoint solve relative to a forward-only solve was estimated empirically across all simulation runs completed. The LHS and PCE methods were applied with varying samples sizes  $N$  as noted above. When MPP reliability methods are used to evaluate multiple probability levels (here, 15 levels for each of mass and dose, for a total of 30 levels), the calculation can be warm-started for each subsequent probability level. So, while a single probability level required 4 forward and 4 adjoint solves, all 30 levels calculated only required 54 forward and 54 adjoint solves in total.

Table II. Cost of UQ studies, relative to cost of one forward transport calculation.

Method	Relative Cost	Notes
MV	1.75	1 forward + 1 adjoint solve
MPP	4 * 1.75	4 * (fwd. + adj.) for a single probability level
	54 * 1.75	54 * (fwd. + adj.) in total for 30 probability levels (see text)
LHS_N; PCEf_N	$N$	$N$ (number of samples) forward solves
PCEg_N	$N * 1.75$	$N$ (number of samples) forward + adjoint solves

Table III summarizes the mean and standard deviation for dose, as calculated by a select subset of the Dakota UQ methods. (Statistics on both mass and dose were computed, but only the more interesting results for dose are presented here. For this problem formulation, mass is exactly linear in the uncertain variables considered and all the methods predict statistics well for it).

Table III. Predicted moments for dose (krad) from select UQ methods.

Method	Mean	Standard Deviation
MV	10.0133	0.3802
PCEg_10	10.0227	0.3809
PCEf_20	10.0220	0.3808
LHS_50	10.0243	0.3979
LHS_3200	10.0229	0.3808

Figures 2 and 3 show cumulative distribution functions (CDFs) resulting from specifying probability levels to various Dakota methods and requesting calculation of the corresponding dose levels. For example, the median dose is 10.0 krad and the probability of the dose being less than 10.9 krad is approximately 99%. From Figure 2 one might conclude that all the UQ methods, save the under-resolved LHS\_50, are in good agreement; indeed, they all agree well near the median. Figure 3 highlights the challenge in predicting upper tail probabilities, where the methods deviate by as much as 0.1 krad.

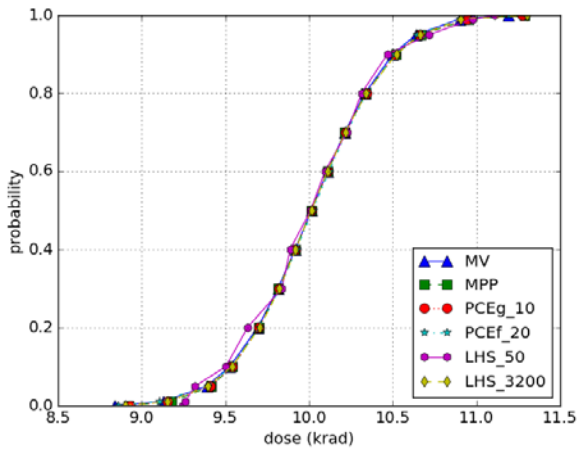


Fig. 2. Cumulative distribution function for dose as a result of several select UQ methods.

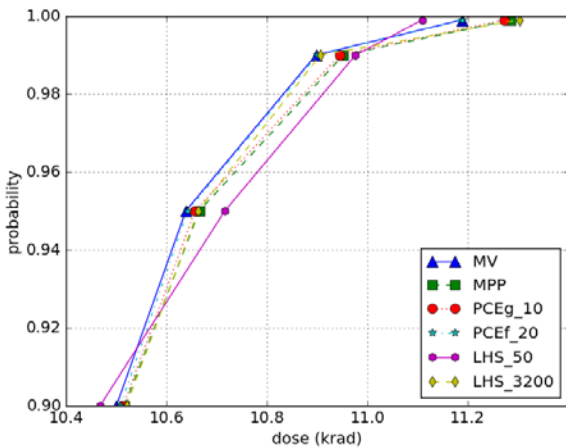


Fig. 3. Cumulative distribution function for dose, emphasizing upper percentiles.

Figures 4, 5, and 6, show the convergence of various methods for the mean, standard deviation, and 99<sup>th</sup> percentile, respectively. For mean and standard deviation, the LHS and PCE methods appear to be converging on the same solution, while for the 99<sup>th</sup> percentile, the LHS is likely still under-resolved. (Dakota's MPP methods cannot calculate moment statistics, so they are omitted.) Both value-only and adjoint-enhanced PCE perform well for this smooth problem, with the gradient-enhanced variant showing a slight computational efficiency advantage. Figure 6 again demonstrates the challenge of estimating a tail probability with sampling methods (unresolved even at 3200 samples), and that the MPP and PCE methods show promise in reliably estimating these quantities with lower computational cost (roughly 4 and 20 model evaluations, respectively).

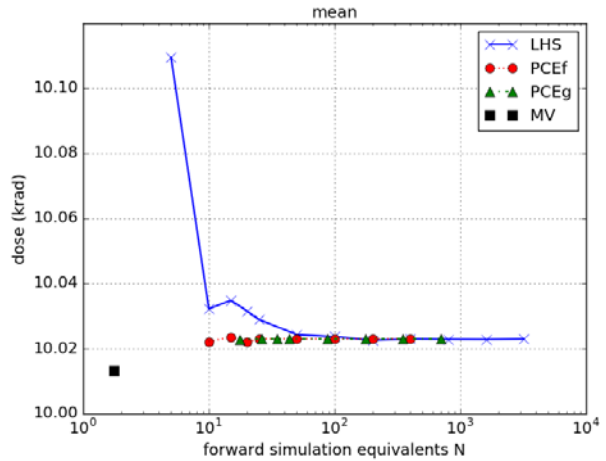


Fig. 4. Convergence of mean dose as a function of simulation cost.

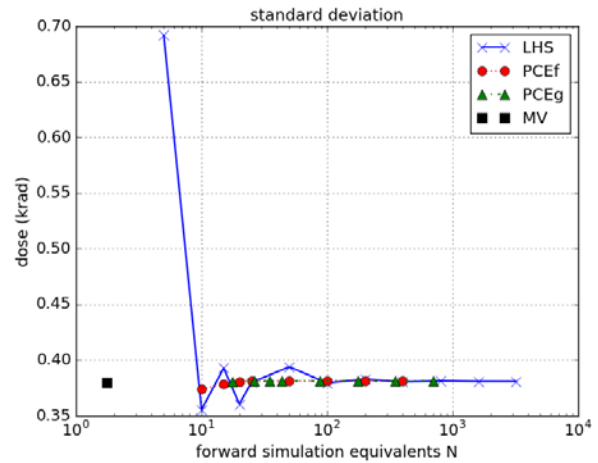


Fig. 5. Convergence of standard deviation of dose as a function of simulation cost.

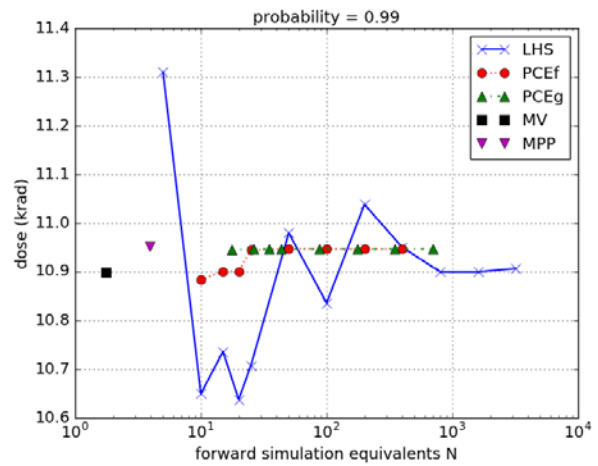


Fig. 6. Convergence of 99<sup>th</sup> percentile of dose as a function of simulation cost.

#### IV. CONCLUSIONS

These preliminary results show promise that gradient-enhanced UQ methods can be more efficient than function value-only approaches in analyzing satellite radiation shields. Advanced reliability and PCE UQ methods can take advantage of adjoint-based sensitivities and calculate more accurate statistics than first-order approximations or Monte Carlo sampling. The performance gains reported here are modest. As we turn our attention to analyses with more complex geometries and transport physics, we hope to see more substantial benefit to the gradient-based MPP reliability and gradient-enhanced PCE methods. Future work will also consider uncertainty in mission source spectrum environment, using the richer characterization available in the AE9/AP9/SPM: Radiation Belt and Space Plasma Specification Models [8].

Our planned work includes enabling risk-informed shield design, where a designer can specify probabilistic performance constraints such as “the probability of dose exceeding 10 krad must be less than 0.001,” or “the mean dose plus three standard deviations must be less than 10.1 krad.” A nested design optimization under uncertainty strategy (Figure 7) can be used to find designs satisfying such probabilistic requirements. Here, for each design proposed by the optimizer, an inner iteration performs UQ on the simulation responses  $g(x; u)$ , resulting in statistics  $s(x)$ . The statistics can be included in objectives or constraints of the outer optimization problem.

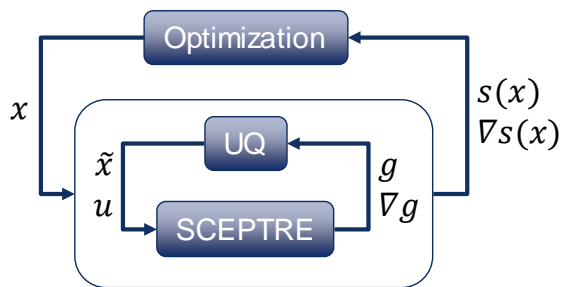


Fig. 7. Depiction of nested design optimization under uncertainty, with analytic design gradients of statistics.

Nested design processes can be prohibitively expensive when each inner iteration requires a Monte Carlo UQ analysis. As previously discussed, our adjoint-enabled transport solver enables more efficient gradient-based UQ methods in the inner loop. In addition, when using gradient-based UQ methods, Dakota can also compute accurate sensitivities of the statistics to the design variables, enabling efficient gradient-based optimization at the outer loop. This will enable risk-informed design at significantly lower cost than sampling-based UQ and enable analysts to directly find optimal designs that meet probabilistic constraints.

#### NOMENCLATURE

- $C$  = collision operator
- $D$  = spatial domain, discrete-to-moment operator
- $E$  = particle energy
- $g$  = response to radiation
- $i$  = simulation evaluation index
- $j$  = basis polynomial index
- $L$  = streaming operator
- $\mathcal{L}$  = Lagrangian
- $m$  = material index
- $\mu_g$  = mean response
- $\Omega$  = particle direction
- $p$  = arbitrary design/uncertain parameter
- $\psi$  = angular flux
- $\psi^\dagger$  = adjoint angular flux
- $q$  = transport source
- $q^\dagger$  = adjoint transport source
- $r$  = spatial coordinate
- $S$  = scattering operator
- $s$  = arbitrary statistic
- $\sigma_d$  = dose cross section
- $\sigma_g$  = response standard deviation
- $\sigma_s$  = scattering cross section
- $\sigma_t$  = total cross section
- $u$  = uncertain variable/parameter
- $x$  = design variable/parameter
- $V$  = volume of region

#### ACKNOWLEDGMENTS

Supported by the Laboratory Directed Research and Development program at Sandia National Laboratories, a multi-mission laboratory managed and operated by Sandia Corporation, a wholly owned subsidiary of Lockheed Martin Corporation, for the U.S. Department of Energy’s National Nuclear Security Administration under contract DE-AC04-94AL85000.

#### REFERENCES

1. W.C. FAN, C.R. DRUMM, S.B. ROESKE, and G.J. SCRIVNER, “Shielding Considerations for Satellite Microelectronics,” *IEEE Trans. On Nuclear Science*, **43**, 6, 2790 (1996).
2. S.D. PAUTZ, B.C. FRANKE, B.M. ADAMS, L.P. SWILER, AND E.L. BLANSETT, “Adjoint-Based Sensitivities for Optimization of Satellite Electron/Proton Shields,” *Proc. ANS M&C 2017*, Jeju, Korea, April 16—20, 2017, American Nuclear Society (2017) (*submitted*).
3. H. F. STRIPLING, M. ANITESCU, and M. L. ADAMS, “A generalized adjoint framework for sensitivity and global error estimation in time-dependent nuclear reactor simulations,” *Annals of Nuclear Energy*, **52**, 47 (2013).

4. D.E. BRUSS, *Adjoint-Based Uncertainty Quantification for Neutron Transport Calculations*, Ph.D. Dissertation, Texas A&M University (2016).
5. S. PAUTZ, B. BOHNHOFF, C. DRUMM AND W. FAN, "Parallel Discrete Ordinates Methods in the SCEPTRE Project," *Proc. Int. Conf. on Mathematics, Computational Methods and Reactor Physics*, Saratoga Springs, NY, May 3-7, 2009, CD-ROM, American Nuclear Society (2009).
6. B.M. ADAMS, et al., "Dakota, A Multilevel Parallel Object-Oriented Framework for Design Optimization, Parameter Estimation, Uncertainty Quantification, and Sensitivity Analysis: Version 6.4 User's Manual," SAND2014-4633, Sandia National Laboratories (2016).
7. "Space Environment Information System (SPENVIS)", <http://www.spennis.oma.be/spennis>, European Space Agency (2016).
8. W. R. JOHNSTON, et al., "AE9/AP9/SPM: New models for radiation belt and space plasma specification," *Proc. SPIE 9085, Sensors and Systems for Space Applications VII*, **908508** (2014).